Dynamic Bipedal Walking by Controlling only the Equilibrium of Intrinsic Elasticities

Dominic Lakatos[1], Alin Albu-Schäffer[1,2],Christian Rode[3] and Florian Loeffl[1]

***Abstract*— This paper presents a methodology for controlling dynamic bipedal walking in a compliantly actuated humanoid robotic system. The approach is such that it exploits the natural leg dynamics of the single and double support phase of the gait. The present approach avoids to close a torque control loop at joint level. While simulation implementations of torque based walking for series elastic actuator (SEA) humanoids display very promising results, several robustness issues very often appear in the experiments. Therefore we introduce here a minimalistic controller, which is based on feedback of control input collocated variables, with the only exception of zero joint torque control. Reshaping of the intrinsic elasticities by control is completely avoided. In order to achieve a coordinated movement of swing and stance leg during single support phase, an appropriate one-dimensional manifold of the motor positions is designed. This constrained behavior is experimentally shown to be compatible with the intrinsic mechanical oscillation mode of the double support phase. The feasibility of this methodology is experimentally validated on a human-scale, anthropomorphic bipedal robotic system with SEA actuation.**

I. Introduction

In contrast to quasi-static walking, where the vertical projection of the center of mass is always inside the support polygon, dynamic walking implies mechanical robustness of the hardware against impacts and high peak forces due to dynamically changing contact situations. Since motors and feasible control loops are not sufficiently fast to react safely against high-frequency impacts, real springs have to be introduced in the power-train between motors and links [1] which together with damping present in any physical system act as low-pass filters on the external forces. In addition to the robustness properties resulting due to the introduction of springs, the elastic energy storages can be exploited to increase the performance and efficiency by exploiting intrinsic resonance properties of the plant. However, besides the beneficial properties, the elastic elements double the order of the dynamics compared to rigid robots which particularly turns the control of dynamical locomotion into a challenging task.

Classical approaches based on the inverted pendulum model and the zero moment point (ZMP) [2], [3], [4] are mainly intended for quasi-static walking gaits. These approaches apply to fully actuated rigid robots which cannot handle high peak forces as potentially appearing in dynamic walking gaits. In order to be able to evolve from static to dynamic walks, the introduction of elastic actuation elements helps to reduce the impact forces and offers energy saving capabilities for weight bearing and the swing motions of the legs [5]. On the basis of these insights, the conceptual spring loaded inverted pendulum (SLIP) models [6], [7], [8], [9] or the compliant hybrid zero dynamics framework [10] have been introduced. Thereby, the template dynamics such as the SLIP model or the hybrid zero dynamics need to be implemented via virtual constraint. These dynamics, substantially differ from the dynamics of a humanoid robot with segmented legs having non-negligible mass. Therefore, the desired SLIP behavior has to be imposed to the plant, e.g., by feedback linearization [10] or virtual model control [11], [12], [13]. These robotic control implementations of legged locomotion hence require to substantially change the dynamics of the plant, which is restricted by actuator limitations.

In this work, we first identify and then excite the natural dynamics of the system during the stance phase. The energy efficient input into the system along the dominant intrinsic oscillation mode is then exploited in the single support phase

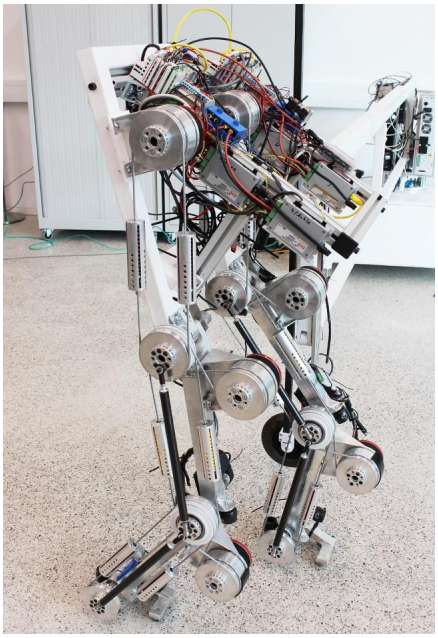

Fig. 1. The DLR C-Runner. A human-scaled bipedal robot with series elastic actuator used for experimental validation of our approach.

[1]D. Lakatos, A. Albu-Schäffer, and F. Loeffl are with the Robotic Mechatronic Center (RMC), Institute of Robotics and Mechatronics, German Aerospace Center (DLR), D-82234 Oberpfaffenhofen, Germany dominic.lakatos@dlr.de

[2]A. Albu-Schäffer is also with Technical University Munich, Chair of Sensor Based Robots and Intelligent Assistance Systems, Department of Informatics, D-85748 Garching, Germany.

[3]C. Rode is with the Department of Motion Science, Friedrich Schiller Universität Jena, D-07749 Jena, Germany.

which is designed by the concept of a one-dimensional manifold. These constraints achieve a coordination of the stance and swing leg dynamics only by feedback of the control input collocated motor positions. Thereby, the required motion of the dynamic walk can be generated without the need of link-side stiffness reshaping which is shown to usually result in positive torque feedback. As a result, the dynamic walking controller is practically feasible as exemplified by experiments.

The paper is structured as follows: Sect. II introduces the basic idea of the controller based on simple examples. In Sect. III the considered model is introduced and the problem of controlling compliantly actuated systems in highly dynamics tasks is stated. The dynamic walking control algorithm is introduced in Sect. IV and experimental validation is provided in Sect. V. Finally, Sect. VI briefly concludes the work.

II. Idea

The basic idea of this paper is to exploit the mechanical robustness and energy efficiency properties of compliant actuators to achieve dynamic and fast bipedal walking in a human-like scaled robotic system.

A. Compliant actuators

The basic principle of compliant actuators is to connect the load to the motor via an elastic element. Thereby, the assembly is such that the motor including gear-box acts via a spring on the link inertia. The simplest model representing a single compliantly actuated joint (in the absence of gravity) can be expressed as

$$M\ddot{q} + D\dot{q} = K\left(\theta - q\right) + \tau_{\text{ext}}\,. \tag{1}$$

Herein, $M > 0$ denotes the inertia of the link, $K > 0$ is the stiffness of a linear spring, $\theta \in \mathbb{R}$ and $q \in \mathbb{R}$ represent the positions of motor and link, respectively, and $\tau_{\text{ext}} \in \mathbb{R}$ is an external torque. Since the elastic element of compliant actuators transmits energy from the motor to the link, an efficient design avoids friction as much as possible such that the dissipative torque $D\dot{q}$ (where $D > 0$) can be assumed to be concentrated at the link-side.

Note that this simple model (1) will be considered to explain the basic mechanisms of mechanical robustness and energy efficiency which are of paramount importance for dynamic bipedal walking, while the full nonlinear model is addressed in the controller design and evaluation.

B. Robustness against impacts

Quasi-static walking implies that the zero moment point (ZMP) is always inside the support polygon, i. e., all trajectories of the gait are such that the system is statically balanced. In contrast, dynamic walking consists of stable and unstable phases. The latter is a result of a transitional under-actuated rigid-body dynamics during the single support phase which corresponds mainly to the inverted pendulum dynamics. The changing contact situations of the dynamic gait lead to impacts which the robotic hardware needs to resist. Compliant actuators are intrinsically robust against corresponding high frequency external torques without requiring the motor to move. This can be seen by inspecting the dynamics (1) under the change of coordinate $\tau = K(\theta - q)$, where the motor position is assumed to be constant, i. e., $\theta = \text{const.}$:

$$MK^{-1}\ddot{\tau} + DK^{-1}\dot{\tau} + \tau = -\tau_{\text{ext}}\,. \tag{2}$$

The resulting relation represents the dynamics of a second order low-pass filter for the external torques τ_{ext}. Peaks of impact forces above the cutoff frequency $\omega_{\text{c}} = \sqrt{K/M}$ are suppressed such that joint torques τ reaching the gear-box do not contain the high peaks of the impact. Thus robustness against impacts is achieved automatically by the elastic elements of compliant actuators.

C. Principles of energy efficient motion generation

To achieve energy efficient motion generation, we exploit very basic control principles which excite the natural dynamics of the plant rather than reshaping it by feedback control. Note that the walking task can be subdivided into the single support phase (i. e., one foot in contact) and the double support phase, each displaying a different dynamics. The former is dominated by the rigid body motion of an inverted pendulum in the gravity field. The latter basically displays a multi degree of freedom dynamics structurally equivalent to the one degree of freedom compliant actuator (1), i. e., dominated by the inertial and compliance effects. Switching the motor position θ by a constant amount $\hat{\theta}$ triggered by a threshold ϵ_τ on the generalized force τ which corresponds to the first oscillation mode of the system [14], i. e.,

$$\theta = \begin{cases} \text{sign}(\tau)\hat{\theta} & \text{if } |\tau| > \epsilon_\tau \\ 0 & \text{otherwise} \end{cases}\,, \tag{3}$$

excites and sustains an asymptotically stable limit cycle of a mass-spring-damper dynamics [15]. The basic idea of this paper is to exploit this fundamental principle for the excitation of a natural oscillation in the double support phase of the gait and then use the gained energy of the oscillation to "overcome the gravity" of the rigid body motion in the single support phase. Thus a coordinated transfer of energy between the two phases is achieved, where each phase performs a natural motion.

D. Static equilibrium control of intrinsic elasticities

Besides the advantageous properties of mechanical robustness and energy efficiency, the introduction of elasticities entails an increase in the order of the plant dynamics compared to rigid robot joints which can be taken into account by considering the motor dynamics[1]

$$B\ddot{\theta} + K\left(\theta - q\right) = u \tag{4}$$

in addition to the link dynamics (1). Herein, $B > 0$ is the constant inertia of the rotor and the motor torque $u \in \mathbb{R}$ is the control input. The additional dynamics[2] (4) due to the

[1]This model implies the classical assumption that the motor and link inertia are not coupled [16], which is valid for common compliantly actuated robots with rotational motors and high gear ratio.

[2]If the control variable of interest is q, the relative degree is four instead of two as for classical rigid robots.

compliant actuation appearing between the control input u and the link side states $q, \dot{q}$ makes the control of compliantly actuated robots a challenging task.

In particular, most of the bipedal locomotion control approaches such as [3], [11], [12], [2], [4], [13], [17], [10] etc. assume a high bandwidth control input either on joint position or joint torque level. However, due to actuator limitations, model parameter uncertainties, noise, and unmodeled dynamics, providing such control inputs in compliantly actuated systems is mainly limited to tasks of slow dynamics (i. e., low frequency tasks). Since we are interested in highly dynamic locomotion, the basic idea of the presented methodology is the use of only control input collocated variables, i. e., $\theta, \dot{\theta}$, in the feedback loops.

III. Problem statement

A. Modeling

We consider compliantly actuated bipedal robotic systems satisfying the free-floating base dynamics

$$\boldsymbol{M}(\boldsymbol{x})\ddot{\boldsymbol{x}} + \boldsymbol{C}(\boldsymbol{x}, \dot{\boldsymbol{x}})\dot{\boldsymbol{x}} + \frac{\partial U_{\mathrm{g}}(\boldsymbol{x})^T}{\partial \boldsymbol{x}} + \begin{pmatrix} \boldsymbol{0} \\ \frac{\partial U_{\mathrm{e}}(\boldsymbol{\theta},\boldsymbol{q})^T}{\partial \boldsymbol{q}} \\ \frac{\partial U_{\mathrm{e}}(\boldsymbol{\theta},\boldsymbol{q})^T}{\partial \boldsymbol{\theta}} \end{pmatrix} = \begin{pmatrix} \boldsymbol{J}_{\mathrm{c}}(\boldsymbol{h},\boldsymbol{q})^T \boldsymbol{\lambda}_{\mathrm{c}} \\ \boldsymbol{u} \end{pmatrix} - \begin{pmatrix} \boldsymbol{0} \\ \boldsymbol{d}(\boldsymbol{q},\boldsymbol{\theta},\dot{\boldsymbol{q}},\dot{\boldsymbol{\theta}}) \end{pmatrix} . \quad (5)$$

Herein, $\boldsymbol{M} \in \mathbb{R}^{(n_{\mathrm{b}}+2n_{\mathrm{j}})\times(n_{\mathrm{b}}+2n_{\mathrm{j}})}$ represents the inertia matrix and $\boldsymbol{C}\dot{\boldsymbol{x}} \in \mathbb{R}^{n_{\mathrm{b}}+2n_{\mathrm{j}}}$ the generalized Coriolis/centrifugal forces. The total potential energy of the system comprises the gravity potential $U_{\mathrm{g}} \in \mathbb{R}$ and the elastic potential $U_{\mathrm{e}}(\boldsymbol{\theta}, \boldsymbol{q}) \in \mathbb{R}$. The latter is assumed to be a convex function in each of its arguments. The configuration variables of the dynamics (5) at position level

$$\boldsymbol{x} = \begin{pmatrix} \boldsymbol{h} \\ \boldsymbol{q} \\ \boldsymbol{\theta} \end{pmatrix} \quad (6)$$

are composed of the configuration of the free-floating base $\boldsymbol{h} \in \mathbb{R}^{n_{\mathrm{b}}}$, the joint positions $\boldsymbol{q} \in \mathbb{R}^{n_{\mathrm{j}}}$ and the motor positions $\boldsymbol{\theta} \in \mathbb{R}^{n_{\mathrm{j}}}$, where n_{b} denotes the number of floating base degrees of freedom and n_{j} the number of (single degree of freedom) joints. Only the states of the motors $\boldsymbol{\theta}, \dot{\boldsymbol{\theta}}$ are directly actuated via the motor torques $\boldsymbol{u}$, which are the only control input of the system. The free-floating base and the link dynamics can be subject to contact forces $\boldsymbol{\lambda}_{\mathrm{c}}$, where $\boldsymbol{J}_{\mathrm{c}}$ is the corresponding Jacobian matrix of the contact points[3]. Finally, the term $\boldsymbol{d} \in \mathbb{R}^{2n_{\mathrm{j}}}$ accounts for the generalized dissipative forces (i. e., friction and damping) which are present in any mechanical system. They are assumed to satisfy

$$\begin{pmatrix} \dot{\boldsymbol{q}}^T & \dot{\boldsymbol{\theta}}^T \end{pmatrix} \boldsymbol{d}(\boldsymbol{q},\boldsymbol{\theta},\dot{\boldsymbol{q}},\dot{\boldsymbol{\theta}}) \geq 0 \, , \forall \dot{\boldsymbol{q}}, \dot{\boldsymbol{\theta}} \in \mathbb{R}^{n_{\mathrm{j}}} .$$

The model (5) is introduced in a very general form since the basic control concepts proposed in this paper apply to such a general model. To simplify the description, we will focus on the specific case of our robotic hardware system in the following. In that case $n_{\mathrm{b}} = 3$ (i. e., the base is free to translate and rotate in the plane), $n_{\mathrm{j}} = 6$ (i. e., single degree of freedom joints for the hip, knee, and ankle of each of the two legs), and the elastic potential is quadratic and such that each joint is actuated via one motor, i. e.

$$U_{\mathrm{e}} = \frac{1}{2} (\boldsymbol{q} - \boldsymbol{\theta})^T \boldsymbol{K} (\boldsymbol{q} - \boldsymbol{\theta}) \, , \quad (7)$$

where $\boldsymbol{K} \in \mathbb{R}^{6\times6}$ is a diagonal and positive stiffness matrix.

B. Avoiding joint torque control

Many locomotion control approaches [12], [13], [17], [10] could be directly applied to plants satisfying (5), if the joint torque $\boldsymbol{\tau} = \boldsymbol{K}(\boldsymbol{\theta} - \boldsymbol{q})$ would be a control input of the system. Since this is not the case, some methods [18], [19] have been investigated to provide a joint torque input by closing an inner control loop. However, as conceptually discussed in Sect. II, closing an inner joint torque control loop could lead to an unstable behavior or limitations in the control performance especially for fast impacts and highly dynamic motions. In the following, this state of affairs will be exemplified formally for the case of reshaping the stiffness seen from the joint outputs.

Assume that we want to reshape the intrinsic joint stiffness of the plant $\boldsymbol{K}$ to the value $\boldsymbol{K}_{\mathrm{des}}$ to match a desired task dynamics, which is different from the intrinsic one. This would be achieved by desired joint torques of the form

$$\boldsymbol{\tau}_{\mathrm{des}} = \boldsymbol{K} (\boldsymbol{\theta}_{\mathrm{des}} - \boldsymbol{q}) = -\boldsymbol{K}_{\mathrm{des}} \boldsymbol{q} \quad (8)$$

or equivalently by desired motor positions of the form

$$\boldsymbol{\theta}_{\mathrm{des}} = \left(\boldsymbol{I} - \boldsymbol{K}^{-1} \boldsymbol{K}_{\mathrm{des}} \right) \boldsymbol{q} \, . \quad (9)$$

Since $\boldsymbol{\theta}_{\mathrm{des}}$ depends on $\boldsymbol{q}$, where $\boldsymbol{q}$ is a system state, $\boldsymbol{\theta}_{\mathrm{des}}$ varies over time. Therefore, a motor position controller of the form

$$\boldsymbol{u} = -\boldsymbol{K}_{\mathrm{P}} (\boldsymbol{\theta} - \boldsymbol{\theta}_{\mathrm{des}}) - \boldsymbol{K}_{\mathrm{D}} \dot{\boldsymbol{\theta}} + \boldsymbol{n}(\dot{\boldsymbol{\theta}}_{\mathrm{des}}, \ddot{\boldsymbol{\theta}}_{\mathrm{des}}, \ldots) \quad (10)$$

would be required to achieve a tracking of $\boldsymbol{\theta}_{\mathrm{des}}$, where $\boldsymbol{K}_{\mathrm{P}}, \boldsymbol{K}_{\mathrm{D}} \in \mathbb{R}^{6\times6}$ are positive definite controller gains and $\boldsymbol{n}$ summarize additional feedforward terms. Inspecting the first term of the control (10):

$$u = -\boldsymbol{K}_{\mathrm{P}} \boldsymbol{\theta} + \boldsymbol{K}_{\mathrm{P}} \left(\boldsymbol{I} - \boldsymbol{K}^{-1} \boldsymbol{K}_{\mathrm{des}} \right) \boldsymbol{q} \, , \quad (11)$$

where (9) has been substituted, it can be immediately seen that feedback of the control input non-collocated variable $\boldsymbol{q}$ appears. In particular, if the desired stiffness is chosen higher than the joint stiffness, i. e., $\boldsymbol{K}_{\mathrm{des}} \succ \boldsymbol{K}$, the coefficient of $\boldsymbol{q}$ in (11) becomes negative, which has the same effect as positive torque feedback.

The implementation of control input non-collocated feedback and in particular positive torque feedback is very sensitive to unmodeled dynamics and sensor noise. High frequency disturbances as appearing in dynamic locomotion tasks drive the systems to their limits which in turn could lead to an unstable behavior. As such, the approach presented

[3]Note that the size of the contact quantities depend on the number and dimension of the contact points.

here will be based mainly only on feedback of control input collocated states $\boldsymbol{\theta}, \dot{\boldsymbol{\theta}}$. The only exception will be "zero torque" control, i. e., $\tau_{\text{des},i} = 0$, for some i, which is uncritical as can be seen from the discussion above.

IV. Dynamic walking controller design

The dynamic walking controller design is a joint result of an appropriate double and single support phase control which both exploit the natural dynamics of the plant on the one hand, but also take into account the limitations available in any hardware system on the other hand.

A. Task coordinates

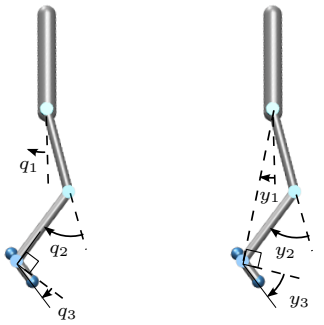

Fig. 2. Task-oriented coordinates for the legs.

Due to the leg segmentation, bipeds and also quadrupeds are able to move in almost every terrain. As a result of this leg structure also the actuation takes place in the joints of the articulated chains of limb segments. However, the locomotion task can be described and analyzed more conveniently in different coordinates than the joint coordinates (cf. the classical inverted pendulum model [3] or the spring loaded inverted pendulum model [6], [7], [8], [9]). Thus, we introduce new task-oriented coordinates which are intended to simplify the synthesis of the walking controller rather than to reshape the original dynamics of the plant. This set of task-oriented coordinates have already partly been used in our previous work [20], but here a simpler representation is introduced, which can be chosen in a singularity free way. A particular extension for the description of bipedal locomotion tasks is presented.

For a single leg with three segments, we identify the following relevant leg task-oriented coordinates as shown in Fig. 2, where the human-inspired assumption of equal thigh and shank segment lengths is made:

1) the angle of the leg $y_1 = q_1 + q_2/2$ which represents the angle between the upper body and the leg axis connecting the center of rotation of the hip and ankle joints,
2) the length of the leg axis $y_2 = l(q_2)$, where $l : \mathbb{R} \to \mathbb{R}$ is a function of q_2 and which represents the distance of the hip and ankle joint rotation axis,
3) the angle of the foot w. r. t. the leg axis $y_3 = q_2/2 + q_3$.

Note that the length of the leg axis could be parameterized by the knee angle itself, i. e., $l(q_2) = q_2$. In that case, the coordinate transformation $\boldsymbol{y} = \boldsymbol{y}(\boldsymbol{q})$ is linear and of course singularity free.

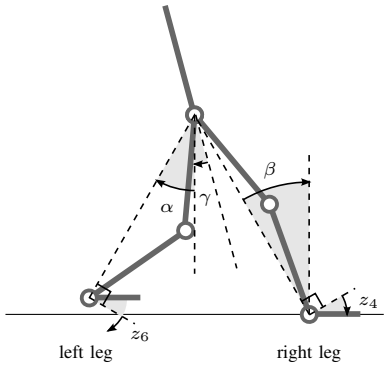

Fig. 3. Bipedal task-oriented coordinates for the hip joints which decouple upper body orientation and the relative leg angle. The angle of the stance leg w. r. t. the vertical line β parameterizes the single support manifold.

On the basis of this leg configuration representation, we can introduce coordinates for the bipedal system which decouple the step length (i. e., the relative leg angle) and orientation of the legs w. r. t. the upper body (see, Fig. 3). Therefore, assume as a first step that the right leg configuration is described by the coordinates (y_1, y_2, y_3) and the left leg configuration by (y_4, y_5, y_6). These configuration variables can be composed as the change of coordinates

$$\boldsymbol{y}(\boldsymbol{q}) = \begin{pmatrix} y_1 \\ y_2 \\ y_3 \\ y_4 \\ y_5 \\ y_6 \end{pmatrix} = \begin{pmatrix} q_1 + \frac{1}{2} q_2 \\ q_2 \\ \frac{1}{2} q_2 + q_3 \\ q_4 + \frac{1}{2} q_5 \\ q_5 \\ \frac{1}{2} q_5 + q_6 \end{pmatrix} \tag{12}$$

between the joint angles $\boldsymbol{q}$ and the leg task-oriented coordinates $\boldsymbol{y}$. Note that in this representation, the coordinate transformation for each leg can be considered separately, i. e., $\boldsymbol{y}_{1\ldots3} = \boldsymbol{y}_{1\ldots3}(\boldsymbol{q}_{1\ldots3})$ and $\boldsymbol{y}_{4\ldots6} = \boldsymbol{y}_{4\ldots6}(\boldsymbol{q}_{4\ldots6})$ for the right and left leg, respectively. Then in a second step, we introduce task-oriented coordinates at a bipedal level. Therefore, we define the relative angle between the leg axes as

$$\alpha = \frac{y_4 - y_1}{2} \tag{13}$$

and the angle between the upper body and the mean angle of the two leg axes as

$$\gamma = \frac{y_1 + y_4}{2} \,. \tag{14}$$

The transformation between the leg and bipedal task-oriented coordinates then takes the form

$$\boldsymbol{z}(\boldsymbol{y}) = \begin{pmatrix} \alpha \\ \gamma \\ z_3 \\ z_4 \\ z_5 \\ z_6 \end{pmatrix} = \begin{pmatrix} \frac{y_4 - y_1}{2} \\ \frac{y_1 + y_4}{2} \\ y_2 \\ y_3 \\ y_5 \\ y_6 \end{pmatrix} . \tag{15}$$

The leg task-oriented coordinates (12) are only introduced as an intermediate derivation step. The complete transformation between the joint and bipedal task-oriented coordinates results by the composition of the mappings (12) and (15):

$$\boldsymbol{z}(\boldsymbol{q}) = \boldsymbol{z} \circ \boldsymbol{y}(\boldsymbol{q}) = \begin{pmatrix} \alpha \\ \gamma \\ z_3 \\ z_4 \\ z_5 \\ z_6 \end{pmatrix} = \begin{pmatrix} \frac{1}{2}\left(q_4 + \frac{1}{2}q_5 - q_1 - \frac{1}{2}q_2\right) \\ \frac{1}{2}\left(q_1 + \frac{1}{2}q_2 + q_4 + \frac{1}{2}q_5\right) \\ q_2 \\ \frac{1}{2}q_2 + q_3 \\ q_5 \\ \frac{1}{2}q_5 + q_6 \end{pmatrix}. \tag{16}$$

These coordinates will form the basis for the controller design presented in the following.

B. Modal motion identification and control

In the double support phase, if the motors hold a constant position, the compliantly actuated system can be deflected w. r. t. its equilibrium position such that a natural oscillation occurs. The oscillation modes exist, in the form defined in linear theory, only for small deflections. However, the first oscillation mode proves to be stably excitable in practice also for oscillations reaching far into the nonlinear regime. Therefore, given an appropriate double support phase configuration [21], and given a stiffness and inertia distribution, the system displays a first oscillation mode which can be exploited to initiate the swing phase of the walking task (see the attached video for an intuitive visualization).

The dominant oscillation modes of the system can be identified by an experiment as described above, where the motors hold a constant position and the motion of the joints is observed. Then, a principal component analysis of the observed data in response to an external perturbation[4]

$$\boldsymbol{Q} = \begin{bmatrix} \boldsymbol{q}(1)^T \\ \boldsymbol{q}(2)^T \\ \vdots \\ \boldsymbol{q}(N)^T \end{bmatrix}, \tag{17}$$

where each of the N rows represents an observation of the oscillation, reveals the averaged direction of the intrinsic mechanical oscillation modes [22]. Thereby, each of the principal vectors corresponds to an oscillation mode. The principal direction with the highest variation, which will be denoted by $\boldsymbol{w}_0 \in \mathbb{R}^{n_j}$, corresponds to the dominant oscillation mode of the plant. This modal motion can be excited and sustained by the adaptive switching law [23]:

$$\boldsymbol{\theta}_{\text{des}} = \boldsymbol{\theta}_0 + \boldsymbol{w}\theta_{\text{w}}\,, \tag{18}$$

where $\boldsymbol{\theta}_0$ represents the initial configuration of the motors and the generalized modal coordinate

$$\theta_{\text{w}} = \begin{cases} \text{sign}(\tau_{\text{w}})\hat{\theta}_{\text{w}} & \text{if } |\tau_{\text{w}}| > \epsilon_{\text{w}} \\ 0 & \text{otherwise} \end{cases} \tag{19}$$

[4]The oscillation modes are an intrinsic property of the plant. Thus, all the following procedures can also be performed in the task-oriented coordinates.

switches with the amplitude $\hat{\theta}_{\text{w}}$ if the generalized modal force $\tau_{\text{w}} = \boldsymbol{w}^T\boldsymbol{\tau}$ overshoots the threshold $\epsilon_{\text{w}} > 0$. Note that thereby given the initial guess $\boldsymbol{w}_0$, the modal weights can be adapted based on the dynamical law

$$\dot{\boldsymbol{w}} = k_{\text{w}}\left(\boldsymbol{w}^T\boldsymbol{q}\right)\left[\boldsymbol{q} - \left(\boldsymbol{w}^T\boldsymbol{q}\right)\boldsymbol{w}\right], \tag{20}$$

where $\boldsymbol{w}(t)$ and $\boldsymbol{q}(t)$ both depend on time and $0 < k_{\text{w}} \ll 1$ represents an adaptation gain [24].

This fundamental principle of natural oscillation excitation can be used to input the kinetic energy required to perform the initial step of the walking gait in a portion wise manner.

C. Single support phase manifold

The single support phase of the walking gait has two main functionalities: (i) the total center of mass has to be borne via the stance leg and transported forward in walking direction and (ii) the swing leg has to be brought to the configuration of the stance leg at the beginning of the double support phase. While (i) can be represented by the dynamics of an inverted pendulum, (ii) could be described by the dynamics of a regular pendulum with the same swing frequency as the inverted pendulum of the stance leg. The coordination of the stance and swing leg motion can be achieved by introducing a constraint which determines the swing leg configuration by means of a parameter describing the state of the stance leg inverted pendulum at position level. Such a parameter could be the absolute angle of the stance leg axis (i. e., the angle between the leg axis and the vertical line, see, Fig. 3). If it is assumed that the stance foot stays flat on the ground, then the angle of the position of the ankle joint can be chosen as parameter. Due to the general concept of avoiding feedback of control input non-collocated variables as discussed in Sect. III-B, the manifold is designed in terms of motor positions which will be denoted by putting a bar on the transformed variables (cf. Sect. IV-A), i. e., $\bar{\boldsymbol{z}} := \boldsymbol{z}(\boldsymbol{\theta})$. Thus, the parameter of the one-dimensional submanifold of $\mathbb{R}^6$ is either $\bar{\beta} = z_4(\boldsymbol{\theta}) = \bar{z}_4$ or $\bar{\beta} = z_6(\boldsymbol{\theta}) = \bar{z}_6$ depending on whether the right or the left leg is the stance leg, respectively. The resulting constraints take the following form:

$$\bar{\boldsymbol{z}}_{\text{des}}^{\text{right}} = \begin{cases} \bar{\alpha}_{\text{des}} &= \bar{\beta} \\ \bar{\gamma}_{\text{des}} &= -h_{3,\text{des}} \\ \bar{z}_{3,\text{des}} &= \rho_0 \\ \bar{z}_{4,\text{des}} &= z_4 + u_\beta \\ \bar{z}_{5,\text{des}} &= \rho_0 + \rho(\bar{\beta}) \\ \bar{z}_{6,\text{des}} &= -\bar{\beta} \end{cases} \tag{21}$$

if the right leg (with joint variables (q_1, q_2, q_3)) is in stance and

$$\bar{\boldsymbol{z}}_{\text{des}}^{\text{left}} = \begin{cases} \bar{\alpha}_{\text{des}} &= -\bar{\beta} \\ \bar{\gamma}_{\text{des}} &= -h_{3,\text{des}} \\ \bar{z}_{3,\text{des}} &= \rho_0 + \rho(\bar{\beta}) \\ \bar{z}_{4,\text{des}} &= -\bar{\beta} \\ \bar{z}_{5,\text{des}} &= \rho_0 \\ \bar{z}_{6,\text{des}} &= z_6 + u_\beta \end{cases} \tag{22}$$

if the left leg (with joint variables (q_4, q_5, q_6)) is in stance. In (21) respectively (22), there appear several constants which parameterize the step:

- $h_{3,\text{des}}$ is the absolute desired orientation of the upper body,
- $\rho_0 > 0$ is the initial knee flexion, and
- u_β is a constant torque offset of the stance foot ankle joint which is realized by a constant deflection of the springs.

Moreover, in (21) respectively (22) the function

$$\rho(\bar{\beta}) = \rho_{\text{flexion}} \cos\left(\max\left(\min\left(\bar{\beta}\alpha_0\pi/2, \alpha_0\right), -\alpha_0\right)\right) \quad (23)$$

which is responsible to ensure ground clearance of the swing leg, is introduced. This function depends on the additional parameters:

- $\alpha_0 > 0$ represents the nominal step length angle and
- $\rho_{\text{flexion}} > 0$ is the additional knee flexion required to ensure ground clearance.

Note that $\bar{z}_{4,\text{des}} = z_4 + u_\beta$ in (21) respectively $\bar{z}_{6,\text{des}} = z_6 + u_\beta$ in (22) implements a "zero torque" control in the ankle joint of the corresponding stance leg. Thereby, u_β is an offset on the "zero torque" which can be used to overcome friction and input the energy required to sustain the gait.

D. Finite state machine

The gait is controlled by a finite state machine which is triggered based on states of the plant at position level. The output of the state machine are desired motor positions $\boldsymbol{\theta}_{\text{des}} = \boldsymbol{z}^{-1}(\bar{\boldsymbol{z}}_{\text{des}})$ which are fed as desired values to the motor PD controller (10) of Sect. III-B.

The state machine comprises two parts: step initiation and continuous walking. The former part implements the modally adaptive limit cycle control (18)–(20). This part is responsible to input the energy required to perform the initial step in a resonance like manner. The second part of the state machine is depicted in Fig. 4. This part of the state machine exploits the symmetry property

$$\bar{\boldsymbol{z}}^{\text{right}}_{\text{des}}(-\bar{\beta}) = \bar{\boldsymbol{z}}^{\text{left}}_{\text{des}}(\bar{\beta}) \quad (24)$$

at the boundary $\bar{\beta} = -\alpha_0$ of the left respectively right leg single support manifold. Under the condition that $u_\beta = 0$ at the transition between the single support manifolds, the desired motor positions $\boldsymbol{\theta}_{\text{des}} = \boldsymbol{z}^{-1}(\bar{\boldsymbol{z}}_{\text{des}})$ are continuous over the complete gait cycle, if the motor position of the corresponding swing leg (i. e., $\bar{z}_4$ respectively $\bar{z}_6$) is tracked appropriately[5]. This can be shown by analyzing the finite state machine that controls the walking gait cycle step-by-step. Therefore, assume that the left leg is initially in stance (cf. state on the bottom of Fig. 4):

- *Left stance phase:* the motion of $\bar{\beta}(\theta_5, \theta_6)$ evolves from α_0 to $-\alpha_0$. When $\bar{\beta}(\theta_5, \theta_6)$ hits the switching boundary given by $\bar{\beta}(\theta_5, \theta_6) = -\alpha_0$, the desired motor positions are held constant at their current value at the switching instance.
- *Right leg retraction:* During this state

$$\bar{\boldsymbol{z}}_{\text{des}} = \bar{\boldsymbol{z}}^{\text{left}}_{\text{des}}(\bar{\beta} = -\alpha_0) = \begin{cases} \bar{\alpha}_{\text{des}} &= \alpha_0 \\ \bar{\gamma}_{\text{des}} &= -h_{3,\text{des}} \\ \bar{z}_{3,\text{des}} &= \rho_0 \\ \bar{z}_{4,\text{des}} &= \alpha_0 \\ \bar{z}_{5,\text{des}} &= \rho_0 \\ \bar{z}_{6,\text{des}} &= -\alpha_0 \end{cases} \quad (25)$$

  holds. Note that $\rho(\bar{\beta} = -\alpha_0) = 0$ has been taken into account (cf. (23)). The touchdown of the actual (right) swing leg triggers the interchange of the leg functionalities, i. e., $\bar{\beta} = -\alpha_0 \to \bar{z}_4$, where $\bar{z}_4 = \alpha_0$ as can be seen in (25).
- *Right stance leg:* It holds

$$\bar{\boldsymbol{z}}_{\text{des}} = \bar{\boldsymbol{z}}^{\text{right}}_{\text{des}}(\bar{\beta} = \alpha_0) = \begin{cases} \bar{\alpha}_{\text{des}} &= \alpha_0 \\ \bar{\gamma}_{\text{des}} &= -h_{3,\text{des}} \\ \bar{z}_{3,\text{des}} &= \rho_0 \\ \bar{z}_{4,\text{des}} &= \alpha_0 \\ \bar{z}_{5,\text{des}} &= \rho_0 \\ \bar{z}_{6,\text{des}} &= -\alpha_0 \end{cases} \quad (26)$$

  at the entry time instance of this state.

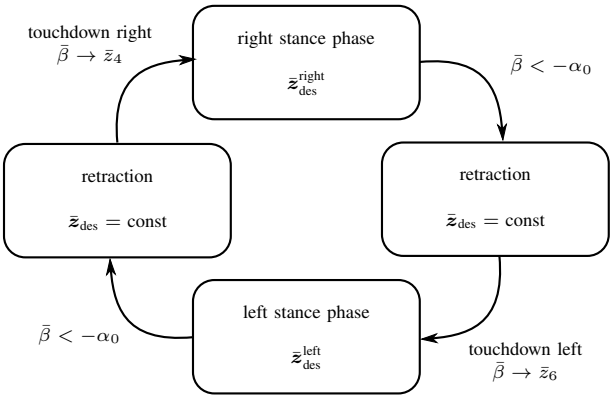

Fig. 4. Finite state machine to control the gait cycle of walking.

By comparing (25) and (26) it can be directly seen that the transition from the left to the right stance leg leads to continuous desired motor positions, under the assumption of ideal motor position tracking, i. e., $\bar{z}_4 = \bar{z}_{4,\text{des}}$ and $\bar{z}_6 = \bar{z}_{6,\text{des}}$[6]. The transition from the right to the left stance leg behaves analogously. Therefore, we may conclude that under the assumption of $u_\beta = 0$, the desired motor positions are continuous for the entire gait cycle.

Remark 1: The step length and consequently the locomotion velocity can be controlled indirectly via the parameter α_0.

Remark 2: The duration of the double support phase can be increased by replacing the touchdown event by triggering

[5]Note that the requirement on the tracking of the swing leg motor positions is rather weak, as the load on this joint is mainly due to its own leg weight.

[6]Note that during the single support phase, the corresponding ankle joint is controlled to "zero torque" and therefore the requirement of ideal tracking is rather weak.

the transition from the retraction to the following single support phase based on the generalized modal force $\tau_w = \boldsymbol{w}^T \boldsymbol{\tau}$, i. e., if $\tau_w > \epsilon_w$ is satisfied. This would lead to a motion along the oscillation mode of the double support phase as discussed in Sect. IV-B. Thereby, the above continuity properties of the desired motor positions are maintained.

Finally, it should be noted that choosing the parameter $u_\beta \neq 0$ leads to a discontinuous switching of the desired motor positions $\bar{\boldsymbol{z}}_{\text{des}}$ which can be used to inject energy for a motion along the single support manifold.

V. Experiments

The goal of the experiments is twofold: first, we want to show that our system displays intrinsic mechanical oscillation modes which can be exploited to initiate a step and which are compatible with the proposed single support phase manifold. Secondly, we aim at validating the proposed dynamic walking control methodology on a real hardware system.

The hardware platform which has been used for the experiments is the DLR C-Runner shown in Fig. 1. It is a planar guided (i. e., the upper body has two translational and one rotational degree of freedom), human-scaled bipedal robot with series elastic actuators. The total body mass is $62\,\text{kg}$ and the outstretched leg length is $0.8\,\text{m}$, where the thigh and shank segment lengths are $0.4\,\text{m}$. Thereby, thigh, shank, and foot have a segment mass of $5.46\,\text{kg}$, $5.42\,\text{kg}$, and $1.31\,\text{kg}$, respectively. Each of the hip, knee, and ankle joints are actuated by a geared electrical motor including a gearbox with transmission ratio of 80, reflected output inertia of $1.6\,\text{kg/m}^2$, maximum output torque of $200\,\text{Nm}$, and maximum output velocity of $5\,\text{rad/s}$. The links are actuated by these drive-units via linear springs with stiffness $500\,\text{Nm/rad}$, $700\,\text{Nm/rad}$, and $500\,\text{Nm/rad}$ for hip, knee, and ankle joint, respectively.

a) Experiment 1: In the first experiment the system has been excited to perform a natural oscillation in a double support configuration using the modally adaptive limit cycle controller of Sect. IV-B. When the oscillation had reached a steady-state, a step based on the approach of Sect. IV-C has been triggered manually by activating a corresponding torque threshold. After performing a complete step, the limit cycle controller was activated again and the whole procedure was repeated. The horizontal motion of the upper body is depicted in Fig. 5. This experimental result[7] reveals that the system displays a natural oscillation mode which is compatible with the single support manifold and can be applied to initiate a dynamic step.

b) Experiment 2: The second experiment shows the continuous dynamic walking control introduced in Sect. IV-D. Thereby, the gait has been initiated by the modally adaptive limit cycle controller of Sect. IV-B. The resulting horizontal motion of the upper body is shown in Fig. 6. Herein it can be seen that the dynamic walk approaches an average velocity of about $1\,\text{m/s}$. As depicted in Fig. 7, the

[7]See also the video of the experiment attached to this paper.

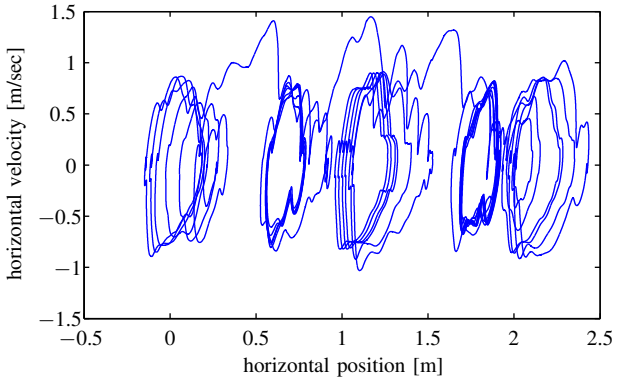

Fig. 5. Phase plot of the horizontal upper body motion. Step initiating modal oscillations and dynamic steps are presented. As the energy of the modal oscillation can be exploited to perform the step, the compatibility of the step and the natural dynamics of the system can be concluded.

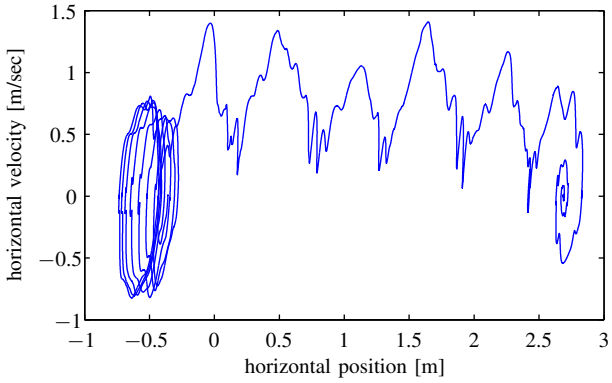

Fig. 6. Phase plot of the horizontal upper body motion. The forward velocity of the upper body of the dynamic walking experiment on the C-Runner hardware is shown over the position. It can be seen that an average velocity of about 1 m/s is achieved

single support manifold parameter $\bar{\beta}(\boldsymbol{\theta})$ is bounded by the control parameter α_0 which indicates the ability to use α_0 for controlling the locomotion velocity. Furthermore, Fig. 8 shows the desired and actual motor positions in terms of the bipedal task-oriented coordinates (15). Thereby, it can be seen that the only discontinuity in the desired motor position arises due to the energy injection $u_\beta < 0$ along the single support manifold. Additionally, it can be seen that our motor position tracking assumption of Sect. IV-D is fulfilled to a large extent. In summary, this experiment is a clear proof of concept of the control methodology presented in this paper[8].

VI. Conclusion

A methodology to control bipedal dynamic walking in a robotic system with series elastic actuators is proposed. The controller implements mainly feedback of control input collocated variables and is therefore robust against unmodeled dynamics and noise. The main part of the controller is a one-dimensional single support manifold implemented on the motor side. The natural dynamics of the plant in the double support phase is shown to be compatible with this

[8]A video showing the dynamic walking experiment is attached to the paper.

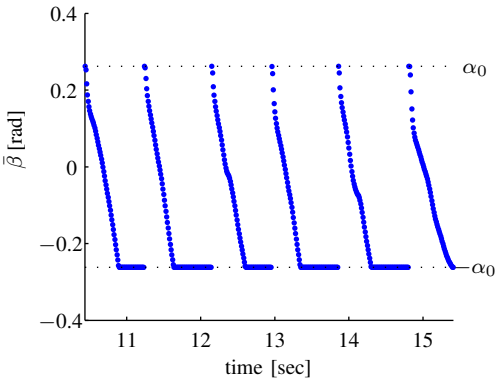

Fig. 7. Time evolution of the single support manifold parameter $\bar{\beta}(\boldsymbol{\theta})$ during the dynamic walking experiment on the C-Runner hardware. It can be observed that $\bar{\beta}(\boldsymbol{\theta})$ is bounded by the control parameter α_0 which influences the step length of the gait.

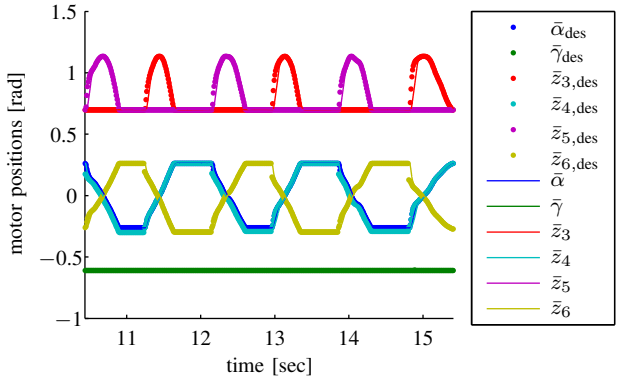

Fig. 8. Desired and actual motor positions in terms of bipedal task-oriented coordinates (15) of the dynamic walking experiment on the C-Runner hardware. The desired values are down-sampled at 100 Hz. The discontinuous switching for inducing energy along the single support manifold can be observed for $\bar{z}_{4,\text{des}}$ and $\bar{z}_{6,\text{des}}$.

single support manifold in a sense that the modal oscillation can be exploited to excite a motion along the single support manifold. A rigorous proof of concept of the approach is given by experiments on a human-scale bipedal robotic hardware.

ACKNOWLEDGMENT

This paper was partly supported by the Helmholtz Association under Grant VH-NG-808.

REFERENCES

[1] G. A. Pratt and M. M. Williamson, "Series elastic actuators," in *Intelligent Robots and Systems 95.'Human Robot Interaction and Cooperative Robots', Proceedings. 1995 IEEE/RSJ International Conference on*, vol. 1. IEEE, 1995, pp. 399–406.

[2] M. Vukobratovic and B. Borovac, "Zero-moment point - thirty five years of its life," *International Journal of Humanoid Robotics*, vol. 2, no. 2, pp. 225–227, 2005.

[3] S. Kajita and K. Tani, "Study of dynamic biped locomotion on rugged terrain-derivation and application of the linear inverted pendulum mode," in *Proc. of IEEE Int. Conf. on Robotics and Automation*, 1991.

[4] P.-B. Wieber, "Trajectory free linear model predictive control for stable walking in the presence of strong perturbations," in *Proc. of IEEE/RAS Int. Conf. on Humanoid Robots*, 2006.

[5] R. M. Alexander, "Three uses for springs in legged locomotion," *International Journal of Robotics Research*, vol. 9, no. 2, pp. 53–61, 1990.

[6] R. Blickhan, "The spring-mass model for running and hopping," *Journal of Biomechanics*, vol. 22, pp. 1217–1227, 1989.

[7] A. Seyfarth, H. Geyer, M. Gnther, and R. Blickhan, "A movement criterion for running." *Journal of Biomechanics*, vol. 35, no. 5, pp. 649–55, 2002.

[8] H. Geyer, A. Seyfarth, and R. Blickhan, "Compliant leg behavior explains basic dynamics of walking and running," *Proceedings of the Royal Society B*, vol. 273, pp. 2861–2867, Nov. 2006.

[9] J. Rummel, Y. Blum, H. M. Maus, C. Rode, and A. Seyfarth, "Stable and robust walking with compliant legs," in *Proc. of IEEE Int. Conf. on Robotics and Automation*, 2010, pp. 5250–5255.

[10] K. Sreenath, H.-W. Park, and J. W. Grizzle, "Embedding active force control within the compliant hybrid zero dynamics to achieve stable, fast running on MABEL," *The International Journal of Robotics Research*, 2013.

[11] J. Pratt, P. Dilworth, and G. Pratt, "Virtual model control of a bipedal walking robot," in *IEEE Int. Conf. on Robotics and Automation*, 1997, pp. 193–198.

[12] J. Pratt and G. Pratt, "Intuitive control of a planar bipedal walking robot," in *IEEE Int. Conf. on Robotics and Automation*, 1998, pp. 2014–2021.

[13] M. Hutter, D. Remy, M. A. Höpflinger, and R. Siegwart, "Slip running with an articulated robotic leg," in *Proc. of IEEE/RSJ Int. Conf. on Intelligent Robots and Systems*, 2010, pp. 4934–4939.

[14] D. Lakatos, F. Petit, and A. Albu-Schäffer, "Nonlinear oscillations for cyclic movements in human and robotic arms," *IEEE Transactions on Robotics*, vol. 30, no. 4, pp. 865–879, 2014.

[15] D. Lakatos and A. Albu-Schäffer, "Switching based limit cycle control for compliantly actuated second-order systems," in *Proceedings of the 19th IFAC World Congress*, 2014, pp. 6392–6399.

[16] M. W. Spong, "Modeling and control of elastic joint robots," *Transactions of the ASME: Journal of Dynamic Systems, Measurement, and Control*, vol. 109, pp. 310–319, 1987.

[17] G. Garofalo, C. Ott, and A. Albu-Schäffer, "Walking control of fully actuated robots based on the bipedal slip model," in *Proc. IEEE Int. Conf. on Robotics and Automation*, 2012, pp. 1999–2004.

[18] C. Ott, A. Albu-Schäffer, A. Kugi, and G. Hirzinger, "Decoupling based cartesian impedance control of flexible joint robots," in *Proc. IEEE Int. Conf. on Robotics and Automation*, 2003.

[19] N. Paine, J. S. Mehling, J. Holley, N. A. Radford, G. Johnson, C.-L. Fok, and L. Sentis, "Actuator control for the nasa-jsc valkyrie humanoid robot: A decoupled dynamics approach for torque control of series elastic robots," *Journal of Field Robotics*, vol. 32, no. 3, pp. 378–396, 2015.

[20] D. Lakatos, C. Rode, A. Seyfarth, and A. Albu-Schffer, "Design and control of compliantly actuated bipedal running robots: Concepts to exploit natural system dynamics," in *2014 IEEE-RAS International Conference on Humanoid Robots*, Nov 2014, pp. 930–937.

[21] D. Lakatos and A. Albu-Schffer, "Modal matching: An approach to natural compliant jumping control," *IEEE Robotics and Automation Letters*, vol. 1, no. 1, pp. 274–281, Jan 2016.

[22] B. Feeny and R. Kappagantu, "On the physical interpretation of proper orthogonal modes in vibrations," *Journal of Sound and Vibration*, vol. 211, pp. 607–616, 1998.

[23] D. Lakatos, M. Görner, F. Petit, A. Dietrich, and A. Albu-Schäffer, "A modally adaptive control for multi-contact cyclic motions in compliantly actuated robotic systems," in *Proc. IEEE/RSJ Int. Conf. on Intelligent Robots and Systems*, 2013, pp. 5388–5395.

[24] E. Oja, "Simplified neuron model as a principal component analyzer," *Journal of mathematical biology*, vol. 15, no. 3, pp. 267–273, 1982.